

Ultrahigh conductivity of large area suspended few layer graphene films

Nima Rouhi, Yung Yu Wang, and Peter J. Burke

Electrical Engineering and Computer Science Department, University of California, Irvine, California 92697, USA

(Received 25 April 2012; accepted 5 December 2012; published online 26 December 2012)

Room-temperature (atmospheric-pressure) electrical conductivity measurements of wafer-scale, large-area suspended (few layer) graphene membranes with areas up to $1000 \mu\text{m}^2$ ($30 \mu\text{m} \times 30 \mu\text{m}$) are presented. Multiple devices on one wafer can be fabricated with high yield from the same chemical vapor deposition grown graphene sheet, transferred from a nickel growth substrate to large opening in a suspended silicon nitride support membrane. This represents areas two to orders of magnitude larger than prior transport studies on any suspended graphene device (single or few layer). We find a sheet conductivity of $\sim 2500 e^2/h$ (or about $10 \Omega/\text{sq}$) of the suspended graphene, which is an order of magnitude higher than any previously reported sheet conductance of few layer graphene.

© 2012 American Institute of Physics. [<http://dx.doi.org/10.1063/1.4772797>]

One of the fundamental unknowns in graphene film transport is the effect of suspending graphene on total conductance. Recent progress in graphene materials synthesis has allowed for large area chemical vapor deposition (CVD) growth, however, progress in large area suspended graphene has been slower. It is well known that the substrate has a dramatic effect on transport properties of single layer graphene,¹ although suspended materials only up to about $1 \times 1 \mu\text{m}$ have been studied to date.²⁻⁴ However, larger size membranes with in-plane electrical transport could enable further studies and applications in a variety of fields, such as optical and electronic devices, mechanical resonators, and chemical and biological sensors.

To date, sub-micron and few-micron (less than $5 \mu\text{m}$) suspended graphene films obtained by mechanical exfoliation and scotch-tape techniques have been demonstrated for material structure studies,⁵⁻⁷ biological membrane and sensing applications,⁸ as mechanical resonators,^{9,10} or pressure chambers.^{11,12} Mechanical resonators built from free-standing epitaxial graphene, up to $20 \mu\text{m} \times 3.5 \mu\text{m}$ size, grown on SiC substrates were also studied.¹³ In addition, large area suspended graphene membranes (up to $100 \mu\text{m}$ in diameter) were fabricated using mechanical exfoliation for thermal conductivity investigations.¹⁴⁻¹⁶ Although mechanically exfoliated graphene provides the highest quality graphene film, the lack in controlling the number of layers, shape, and position of the film on the substrate is a drawback of such a technique.

Using CVD growth techniques (on Ni or Cu), 2–30 μm (both width and length) suspended graphene films were fabricated and mechanical and thermal properties of such membranes were studied extensively.¹⁷⁻²⁰ However, the absence of metallic contacts in most of these studies prevented the characterization of electronic properties of such suspended membranes. Low temperature ($\sim 4 \text{K}$), in-vacuum measurement of electrical characteristics in suspended graphene with very small sizes ($0.1-3 \mu\text{m}$ in length and width)²¹⁻²³ and temperature-dependence of transport in suspended graphene films²⁴ all obtained from mechanical exfoliation have been presented to study improved mobility of suspended graphene. However, the suspended graphene was obtained

through a wet etching of substrate underneath graphene after the deposition of the film and therefore the substrate/graphene interface contamination should be removed through another thermal process as described in Ref. 21. Another study reports few-layer graphene (FLG) grown on Ni and suspended over a $2.5 \mu\text{m}$ diameter hole.²⁵ Thus, to date, electrical transport measurements of suspended graphene have been limited to very small sample sizes, in spite of the large areas available through CVD growth techniques.

In this work, the room-temperature (atmospheric-pressure condition) electrical conductivity measurement of wafer-scale, large-area suspended (few layer) graphene membranes with areas up to $1000 \mu\text{m}^2$ is presented. This represents areas two to orders of magnitude larger than prior transport studies on any suspended graphene device (single or few layer). We find a sheet conductivity of $\sim 2500 e^2/h$ of the suspended graphene, which is two orders of magnitude higher than the graphene from the same sheet on a solid substrate.

The wafer-scale device schematic is indicated in Fig. 1. A silicon substrate with 300 nm LPCVD (low pressure CVD) low-stress nitride cap was etched (using hot KOH) through the backside to make arrays of nitride membranes. Using reactive ion etching (RIE) technique, square holes of 5×5 , 20×20 , and $30 \times 30 \mu\text{m}^2$ were opened at the center of each nitride membrane. Few-layer graphene film is synthesized via low-pressure chemical vapor deposition on Ni.²⁶ Few-layer graphene was then transferred to the silicon nitride membrane where it is freely suspended over the openings in the nitride.

Conventional photolithography followed by e-beam evaporation and lift-off process defines the electrodes (Palladium/Gold (Pd/Au 10:50 nm)). Fig. 2(a) shows the Raman spectrum of few-layer graphene deposited (inset: scanning electron microscopy (SEM) image of a test sample, prepared under the same process used to make other samples in this manuscript, showing a suspended graphene film covering a $\sim 5 \mu\text{m}$ hole and intact at the end of the fabrication process). Fig. 2(b) demonstrates the I-V curve for different hole sizes showing different resistance.

In our experiments, 7 membranes were fabricated and the transfer process was done covering all but one of the

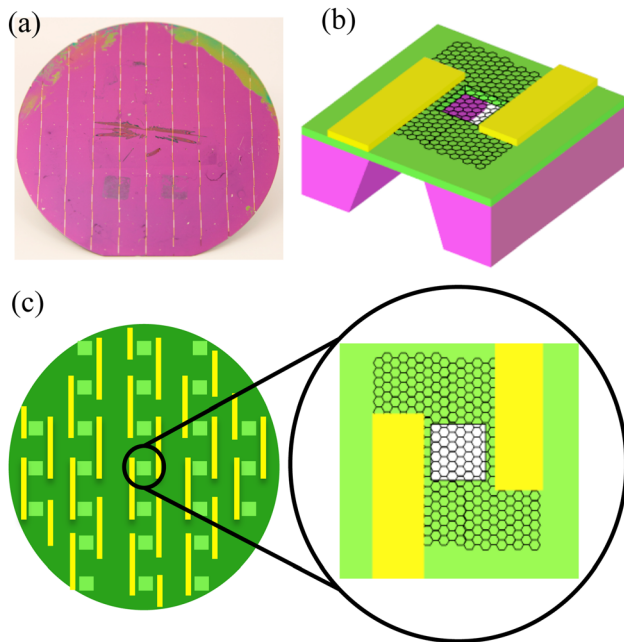


FIG. 1. (a) Optical image of wafer-scale fabrication with actual devices. (b) 3D schematic of a single device design with graphene film partially suspended between electrodes. (c) Top view of large-scale fabrication and zoomed-in single device.

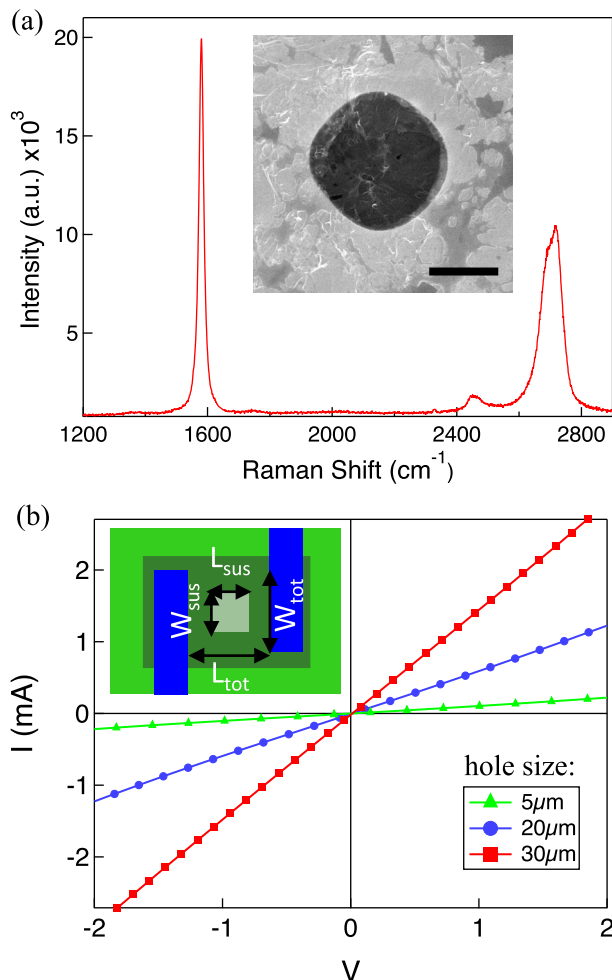


FIG. 2. (a) Raman spectrum of few layer graphene with 2D, G, and D peaks. In the inset; SEM image of suspended graphene film, scale bar is $2 \mu\text{m}$. (b) Current-voltage curve for different hole sizes demonstrating different conductivity depending on hole size, and schematic of a single device.

holes, for yield of 85%. Graphene films are all from one batch with the same growth parameter and cut in $\sim 1 \text{ cm}$ size sheets prior to transfer. Electrical measurements on 6 good membranes (2 for each hole size) show a conductance within the 50% for each membrane size (2 of each size).

In our measurement geometry, both the suspended graphene and the graphene on the substrate (which we call the supported graphene) are both measured in parallel (Fig. 1). Therefore, the conductance measurement of a single sample alone cannot determine the relative contributions of the suspended vs. supported graphene to the total measured conductance.

In order to infer the sheet conductivity of the suspended graphene, a simple model, which assumes the conductivity is independent of the area, has been developed. As it can be seen from Fig. 1 top view, the channel area with graphene film can be divided into 3 different regions: two are the upper and lower sides of the membrane with similar dimensions, (therefore, similar conductance and we count them as one conductor with the width of $W_{\text{tot}} - W_{\text{sus}}$ and length of L_{tot}) and one area which includes the freely suspended membrane with the width of W_{sus} and the left/right sides of membrane up to the electrodes. Each section is then modeled as a resistor/conductor, which is in parallel with other sections and extended from one electrode to another. However, the middle part includes the suspended area and the unsupported area on the left and right of it. Using this model, the total conductance is given by

$$G = \sigma_N \left(\frac{W_{\text{tot}} - W_{\text{sus}}}{L_{\text{tot}}} \right) + \frac{1}{\frac{1}{\sigma_{\text{sus}}} + \frac{1}{\sigma_N} \frac{L_{\text{tot}} - L_{\text{sus}}}{W_{\text{sus}}}}, \quad (1)$$

where σ_N and σ_{sus} are the conductivities of graphene film on nitride substrate and suspended membrane, respectively. L_{tot} is the distance between the electrodes and W_{tot} is the width of electrodes facing each other. L_{sus} is suspended graphene membrane length and in our design, $W_{\text{sus}} = L_{\text{sus}}$ (the suspended area was designed as square). The contribution of possible graphene film extension to the outside of $W_{\text{tot}} \times L_{\text{tot}}$ area is negligible comparing to the total conductance.

In our experiments, the total number of squares (i.e., $L_{\text{tot}}/W_{\text{tot}}$) was approximately the same for all 3 sample sizes, and therefore the total conductance would be the same if the suspended and supported graphene had the same conductance. However, as shown in Fig. 3, the conductance depends strongly on the fraction of the area occupied by the suspended graphene, changing by an order of magnitude. This is clear indication of the high conductance of the suspended graphene relative to the supported graphene.

In order to be more quantitative, we use Eq. (1) above fit to our set of transport data for three different device sizes to infer the conductivity of the suspended and supported graphene. Using this method, we find the conductivity of graphene on nitride substrate (σ_N) is $\sim 20 e^2/h$ while the conductivity of the suspended area (σ_{sus}) is $\sim 2500 e^2/h$. This clearly shows more than $120\times$ sheet conductivity improvement from unsupported to suspended area *within the same film*.

While there have been no other measurements in the literature of the conductivity of suspended FLG, we can

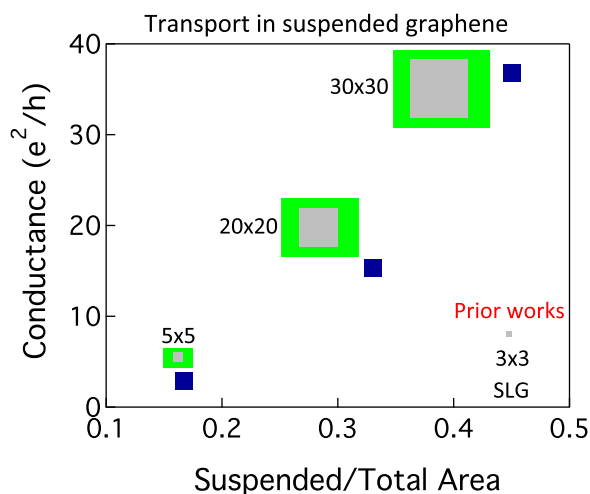


FIG. 3. Normalized conductance of few-layer graphene film as a function of suspended/total area ratio. The green area is graphene on nitride membrane and gray is the suspended graphene scaled for our samples. Conductance increases with increase in suspended/total area ratio. “Prior works” (see Refs. 21 and 22) show relative size of suspended graphene compared to our samples in this figure (sizes are in μm).

compare our results to that of supported FLG. The measured sheet resistance of our suspended graphene ($\sim 10 \Omega/\text{sq}$) is about an order of magnitude lower than that of FLG graphene synthesized on Ni by CVD measured on solid substrates by two other research groups,^{27,28} who found varying sheet resistances typically around $250 \Omega/\text{sq}$ or higher. The mechanism for such an increased conductance is believed to be related to decreased substrate related scattering, however, it should be noted that domain size, density of defects, impurities, and other material properties have significant impact on the conductivity of graphene film which should be taken into account for more precise comparison. In addition, detailed theoretical models for multi-layer graphene have yet to be developed.

The ability to fabricate high conductance suspended graphene films can open the door to many potential applications. Of particular interest is the integration of graphene films with electrochemistry, nanopores, and DNA sequencing, a future application that holds much promise for the use of graphene films.⁸

This work was funded by the Army Research Office through ARO-MURI program and ARO-Core grants (MURI W911NF-11-1-0024, ARO W911NF-09-1-0319, and DURIP W911NF-11-1-0315).

- ¹J. Sabio, C. Seoanez, S. Fratini, F. Guinea, A. H. Castro, and F. Sols, *Phys. Rev. B* **77**(19), 195409 (2008).
- ²K. S. Novoselov, A. K. Geim, S. V. Morozov, D. Jiang, M. I. Katsnelson, I. V. Grigorieva, S. V. Dubonos, and A. A. Firsov, *Nature (London)* **438**(7065), 197 (2005).
- ³A. E. Curtin, M. S. Fuhrer, J. L. Tedesco, R. L. Myers-Ward, C. R. Eddy, and D. K. Gaskill, *Appl. Phys. Lett.* **98**(24), 243111 (2011).
- ⁴J. H. Chen, C. Jang, S. D. Xiao, M. Ishigami, and M. S. Fuhrer, *Nat. Nanotechnol.* **3**(4), 206 (2008).
- ⁵J. C. Meyer, A. K. Geim, M. I. Katsnelson, K. S. Novoselov, T. J. Booth, and S. Roth, *Nature (London)* **446**(7131), 60 (2007).
- ⁶J. C. Meyer, A. K. Geim, M. I. Katsnelson, K. S. Novoselov, D. Obergfell, S. Roth, C. Girit, and A. Zettl, *Solid State Commun.* **143**(1-2), 101 (2007).
- ⁷J. C. Meyer, C. O. Girit, M. F. Crommie, and A. Zettl, *Appl. Phys. Lett.* **92**(12), 123110 (2008).
- ⁸B. M. Venkatesan and R. Bashir, *Nat. Nanotechnol.* **6**(10), 615 (2011).
- ⁹J. S. Bunch, A. M. van der Zande, S. S. Verbridge, I. W. Frank, D. M. Tanenbaum, J. M. Parpia, H. G. Craighead, and P. L. McEuen, *Science* **315**(5811), 490 (2007).
- ¹⁰M. Poot and H. S. J. van der Zant, *Appl. Phys. Lett.* **92**(6), 63111 (2008).
- ¹¹J. S. Bunch, S. S. Verbridge, J. S. Alden, A. M. van der Zande, J. M. Parpia, H. G. Craighead, and P. L. McEuen, *Nano Lett.* **8**(8), 2458 (2008).
- ¹²S. P. Koenig, N. G. Boddeti, M. L. Dunn, and J. S. Bunch, *Nat. Nanotechnol.* **6**(9), 543 (2011).
- ¹³S. Shivaraman, R. A. Barton, X. Yu, J. Alden, L. Herman, M. V. S. Chandrashekar, J. Park, P. L. McEuen, J. M. Parpia, H. G. Craighead, and M. G. Spencer, *Nano Lett.* **9**(9), 3100 (2009).
- ¹⁴A. A. Balandin, S. Ghosh, W. Z. Bao, I. Calizo, D. Teweldebrhan, F. Miao, and C. N. Lau, *Nano Lett.* **8**(3), 902 (2008).
- ¹⁵T. J. Booth, P. Blake, R. R. Nair, D. Jiang, E. W. Hill, U. Bangert, A. Bleloch, M. Gass, K. S. Novoselov, M. I. Katsnelson, and A. K. Geim, *Nano Lett.* **8**(8), 2442 (2008).
- ¹⁶C. Faugeras, B. Faugeras, M. Orlita, M. Potemski, R. R. Nair, and A. K. Geim, *ACS Nano* **4**(4), 1889 (2010).
- ¹⁷W. W. Cai, A. L. Moore, Y. W. Zhu, X. S. Li, S. S. Chen, L. Shi, and R. S. Ruoff, *Nano Lett.* **10**(5), 1645 (2010).
- ¹⁸A. M. van der Zande, R. A. Barton, J. S. Alden, C. S. Ruiz-Vargas, W. S. Whitney, P. H. Q. Pham, J. Park, J. M. Parpia, H. G. Craighead, and P. L. McEuen, *Nano Lett.* **10**(12), 4869 (2010).
- ¹⁹S. S. Chen, A. L. Moore, W. W. Cai, J. W. Suk, J. H. An, C. Mishra, C. Amos, C. W. Magnuson, J. Y. Kang, L. Shi, and R. S. Ruoff, *ACS Nano* **5**(1), 321 (2011).
- ²⁰R. A. Barton, B. Ilic, A. M. van der Zande, W. S. Whitney, P. L. McEuen, J. M. Parpia, and H. G. Craighead, *Nano Lett.* **11**(3), 1232 (2011).
- ²¹K. I. Bolotin, K. J. Sikes, Z. Jiang, M. Klima, G. Fudenberg, J. Hone, P. Kim, and H. L. Stormer, *Solid State Commun.* **146**(9-10), 351 (2008).
- ²²X. Du, I. Skachko, A. Barker, and E. Y. Andrei, *Nat. Nanotechnol.* **3**(8), 491 (2008).
- ²³N. Tombros, A. Veligura, J. Junesch, M. H. D. Guimaraes, I. J. Vera-Marun, H. T. Jonkman, and B. J. van Wees, *Nat. Phys.* **7**(9), 697 (2011).
- ²⁴K. I. Bolotin, K. J. Sikes, J. Hone, H. L. Stormer, and P. Kim, *Phys. Rev. Lett.* **101**(9), 96802 (2008).
- ²⁵W. W. Cai, Y. W. Zhu, X. S. Li, R. D. Piner, and R. S. Ruoff, *Appl. Phys. Lett.* **95**(12), 123115 (2009).
- ²⁶A. Reina, X. T. Jia, J. Ho, D. Nezich, H. B. Son, V. Bulovic, M. S. Dresselhaus, and J. Kong, *Nano Lett.* **9**(1), 30 (2009).
- ²⁷K. S. Kim, Y. Zhao, H. Jang, S. Y. Lee, J. M. Kim, K. S. Kim, J. H. Ahn, P. Kim, J. Y. Choi, and B. H. Hong, *Nature (London)* **457**(7230), 706 (2009).
- ²⁸X. S. Li, Y. W. Zhu, W. W. Cai, M. Borysiak, B. Y. Han, D. Chen, R. D. Piner, L. Colombo, and R. S. Ruoff, *Nano Lett.* **9**(12), 4359 (2009).